Forming Limit Diagram Test of Press Hardening Steel Sheet at Elevated Temperatures

J. P. Zhang(✉), G. Fang, J. Zhou, W. Xu, and M. T. Ma

China Automotive Engineering Research Institute Co., Ltd., Chongqing 401122, China
zhangjunping@caeri.com.cn

Abstract. To investigate the formability of press hardening steel sheet at elevated temperatures, the typical steel sheet 22MnB5 was adopted and tested via a self-designed setup which comprised of a resistance wire oven, a set of punching die and a loading system. Nine specimens were applied to get different strain path. Each specimen was heated in the oven and transferred to the punching die. The temperature was set to 500 °C, 600 °C and 700 °C respectively in the forming process. After experiments, the critical strains and the safe strains were measured and the forming limit curve was created according to the strain distribution.

Keywords: Press hardening steel sheet · Forming limit diagram · Elevated temperatures · 22MnB5

1 Introduction

Over the past decades, the hot press hardening steel sheets are widely applied in the automotive key components such as B-pillar, front and back bumper, etc., due to the effect that helps reduce the weight of body in white and at the same time increase the protect potentials when collision happens [1–3]. In the manufacture process, the sheet is heated to the austenitization temperature in the furnace and transferred to the hot press die. The duration is less than 10 s. The blank is stamped to the component and the microstructure transforms from ferrite and pearlite to martensite, which will dramatically improve the strength of the material accordingly [1, 4, 5].

Typically the formability of the materials in room temperature is depicted by forming limit diagram which is composed of a series of critical strains in different strain paths. There are tons of researches exhibit how to carry out the experiments and obtain the strain points [6–9]. The test setups are also commercially manufactured for sale such as ZWICK BUP sheet forming machine and ERICHSEN forming machine. However, there are rarely setups and no standards for the test of forming limit diagram (FLD) of the hot pressed steel sheet at elevated temperatures. Considering the necessity of the property for hot forming, the present work designs a setup to carry out punching tests at elevated temperatures and establishes data processing and analyzing method. The formability at elevated temperature of the typical hot press hardening steel 22MnB5 is evaluated on this basis.

Y. Zhang and M. Ma (Eds.): ICHSU 2022, AHMST 2, pp. 76–83, 2023.
https://doi.org/10.2991/978-94-6463-114-2_11

2 Experiments

2.1 Materials

The 22MnB5 sheet with the thickness of 1.5 mm was used in the paper. Its chemical compositions and mechanical property are listed in the Table 1 and Table 2 respectively.

2.2 Setups

In order to meet the requirements of high temperature bulging, a high temperature FLD test device (as shown in Fig. 1) is designed and manufactured. The lower end of the device is fixed by bolts, and the upper end is connected with a 20 t oil cylinder. During the test, bulging and blank holder force are applied through the action of the oil cylinder. The main part of the sample device is processed according to the die size recommended in GB15825-2008, and the punch diameter is 100 mm. The equipment mainly has the following characteristics:

(1) Blank holder force adjustment. Install nitrogen spring at the lower part of the device, and provide variable blank holder force to the sample through nitrogen spring compression.
(2) Temperature control. Four heating rods are embedded in the punch and the upper and lower pressing plates respectively. The heating rods are connected with the heating controller. At the time of test, the temperature of the punch and pressing plate is controlled at 25 °C–800 °C through the heating controller.
(3) Measurement of sample temperature. Place an infrared temperature probe at position 3 in the figure to monitor the temperature change of the sample or punch in real time. Water channels are opened in some areas for cooling (Fig. 2).

2.3 Specimens

In this experiment, rectangular samples with length of 188.5 mm and width of 180 mm, 160 mm, 140 mm, 120 mm, 100 mm, 80 mm, 60 mm, 40 mm and 20 mm are used. The

Table 1. The chemical compositions of 22MnB5 (wt.%).

C	Si	Mn	P	S	Cr	Mo	B	Ti	Al
0.23	0.17	0.95	0.01	0.002	0.24	0.21	0.002	0.023	0.03

Table 2. The mechanical property of 22MnB5.

Yield strength ($R_{p0.2}$/MPa)	Tensile strength (R_b/MPa)	Fracture strain (%)
384	566	27.3

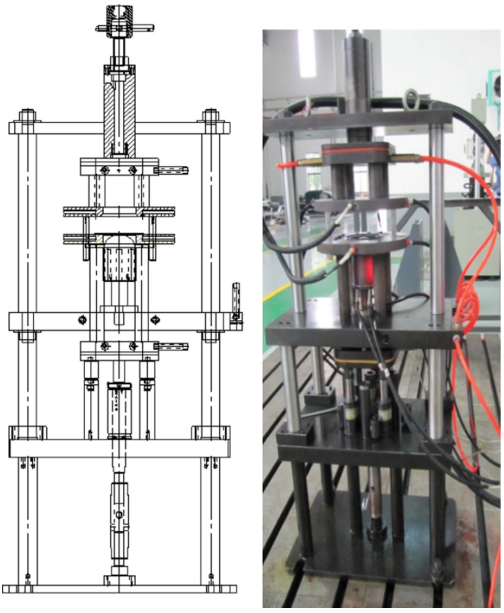

Fig. 1. The schematic drawing and the real picture of the die.

Fig. 2. High temperature FLD test setup, furnace and activator.

sampling direction is perpendicular to the rolling direction, and three samples are taken for each size. In order to prevent the side of the rectangular specimen from cracking at the drawing rib of the die or the notch of the die, the shape of the rectangular specimen is changed into a ladder shape with a slightly narrow middle and widened both ends, or other shapes similar to dumbbells, following the example of the sheet metal tensile specimen. In order to ensure the alignment between the sample and the punch during

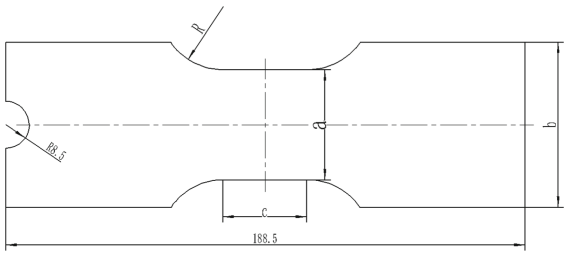

Fig. 3. Specimens for high temperature FLD.

Table 3. Specimen size for high temperature FLD (unit: mm).

a	20	40	60	80	100	120	140	160	180
b	40	60	80	100	120	120	140	160	180
c	32	32	32	32	32	0	0	0	0
R	20	20	20	20	20	0	0	0	0

the test, a semicircle with an arc radius of 8.5 mm is machined at one end of the sample for positioning. The shape and size of the sample are shown in Fig. 3 and Table 3 respectively. Circular grid of 2 mm is carved on the sample by laser engraving for strain measurement.

2.4 Experimental Procedure

Before the test, one side of the sample is engraved with 2 mm circular grid. Then the sample is heated in the high-temperature test box furnace. The target heating temperature is 930 °C for the material. In heating process, the furnace was full of the protective gas to protect the sheet from oxidation, which is comprised of 97% N_2 and 3% H_2. The specimen is heated in the furnace for 300 s and then rapidly transferred to the dies.

In the deformation, there's no any lubrication between the specimen and the punch. The specimen is clamped and punched with the loading speed of 5 mm/s when the temperature decreases to the target temperature. When the crack happens in the surface stop the test. After the sample cooling, the strains are measured and analyzed.

3 Results

The temperature change of the sample during high temperature forming is shown in Fig. 4. It can be seen from the figure that the temperature of samples with different widths has the same downward trend during the test. The wider the width is, the smaller the temperature reduction rate of the sample exhibits. For the same sample, the temperature drop rate is the highest in 10 s after moving out of the furnace. At 600 °C, a platform appears on the temperature drop curve, and the temperature is stable for a period of time in this range. This is because the latent heat of phase change after the material

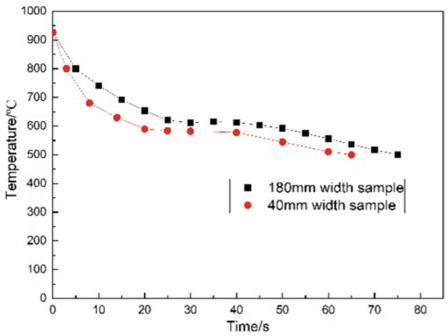

Fig. 4. The temperature trends of the specimen during the test.

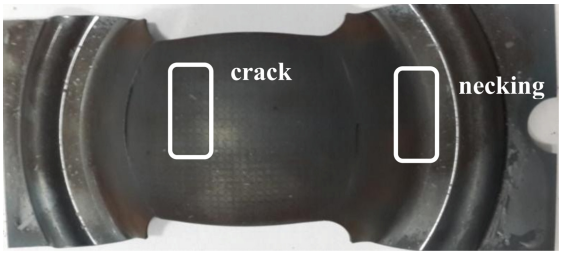

Fig. 5. The specimen after deformation.

changes makes up for the heat loss of the sample in the air. Subsequently, the temperature continued to decline, and its decline rate was significantly lower than that at the time of leaving the furnace.

Since no lubricant is used in the test, double necking phenomena has appeared in the specimen due to the fierce friction effect in the hot punching process. As shown in Fig. 5, the deformation is concentrated on the two sides of the specimen, which are away from the dome. As the punch moves upwards to some extent, cracking occurs on the necked side of the sample, while only necking occurred on the other side (no cracking). Looking specifically in the necking area, a very obvious necking line could be found (as shown in Fig. 6). For those grids crossed by the line, serious deformation makes the grid largely elongated. Therefore, the necked grids are selected as critical grid. By measuring the length of the grids in the long axis direction and in the short axis direction, the critical major strain and minor strain could be calculated referring the original grid size. Commonly, the grids adjacent to the critical grids might experience some extent deformation, but necking feature is not found, which means they are safe for bearing further deformation. Therefore, these grids are called safe grids. Similarly, the safe major strain and minor strain could be obtained.

By collecting the critical grids strain and safe grids strain of all the specimens, the strain distribution could be drawn. As usually, the minor strain is set as x axis while the major strain is denoted as y axis. After drawing the limit strain, the forming limit curve could be drawn as the boundary line between the limit strain at the necking point and the

Fig. 6. Grid deformation and selection in the necking range.

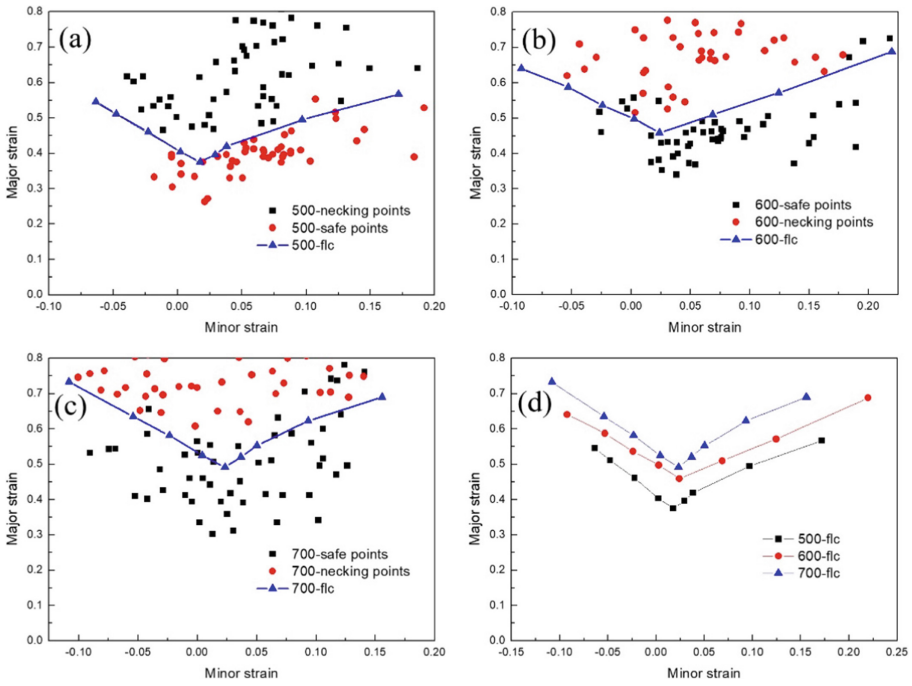

Fig. 7. FLD of the 22MnB5: (a) 500 °C; (b) 600 °C; (c) 700 °C; (d) at three different temperatures.

limit strain at the safety point. FLDs of 22MnB5 under different temperature conditions are shown in Fig. 7, which are comprised of necking points, safe points and forming limit curve (FLC). The left half of the FLC is divided into safety and necking areas by a straight line, and the right half is divided into safety and necking areas by a straight line or curve.

For each forming limit diagram, the strain points exhibit random distribution to some extent. This is because the measurement of the strain is off-line, which means different grids represent different deformation state and degree. Therefore, some grids show extremely large strain, while some grids' strains are very close to the curve. However, by counting large number of safe and critical grids, the intrinsic forming limit of the

material will always be found. As shown in Fig. 7(d), deformation of the material at higher temperature exhibits better formability. The curve at 700 °C is highest while the lowest curve is found at 500 °C.

4 Conclusion

Formability at elevated temperatures is essential for hot press hardening steel sheet. However, the test method and setups are not available for the time being. In the light of this, the present work designs a setup comprised of a resistance wire oven, a set of punching die and a loading system, which could realize high temperature heating and punching. At the same time, the test procedure to simulate the hot process is pointed out and the strain measurement and forming limit diagram drawing methods are created. To ensure the test serviceable, the typical steel sheet 22MnB5 with thickness of 1.5 mm is adopted and tested via the self-designed setup and procedure. The forming limit diagrams of the material at different temperature are obtained. The results show that increasing temperature is beneficial for the hot stamping deformation of the material. The material exhibits better formability at higher temperature.

References

1. K. Karhausen and R. Kopp, Model for integrated process and microstructure simulation in hot forming, *Steel Research* **63**, 247 (1992).
2. M. Merklein, J. Lechler and M. Geiger, Characterisation of the flow properties of the quenchenable ultra high strength steel 22MnB5, *CIRP Annals* **55**, 229 (2006).
3. M. Naderi, L. Durrenberger and A. Molinari, Constitutive relationships for 22MnB5 boron steel deformed isothermally at high temperatures, *Materials Science and Engineering*: A **478**, 130 (2008).
4. R. George, A. Bardelcik and M. J. Worswick, Hot forming of boron steels using heated and cooled tooling for tailored properties, *Journal of Materials Processing Technology* **212**, 2386 (2012).
5. Y. H. Guo and M. T. Ma, Study on the Experiment of Hot Stamping for Front Bumper, *Chinese Engineering Science* **16**, 76 (2014).
6. E. M. Viatkina, W. A. M. Brekelmans and M. G. D. Geers, Forming limit diagrams for sheet deformation processes, *Mate Poster Award 2001: 6th Annual*, (Poster Contest, 2001).
7. S. K. Paul, Controlling factors of forming limit curve A review, A*dvances in Industrial and Manufacturing Engineering* **2**, 100033 (2021).
8. V.C. Do, Q.T. Pham and Y. S. Kim, Identification of forming limit curve at fracture in incremental sheet forming. *The International Journal of Advanced Manufacturing Technology* **92**, 4445 (2017).
9. H. B. Campos, M. C. Butuc, J. J. Gracio, J. E. Rocha and J. M. F. Duarte, Theoretical and experimental determination of the forming limit diagram for the AISI 304 stainless steel, *Journal of Materials Processing Technology* **179**, 56 (2006).